Prewavy instability of nematic liquid crystals in a high-frequency electric field

Jong-Hoon Huh
Department of Mechanical Systems Engineering, Faculty of Computer Science and Systems Engineering, Kyushu Institute of Technology, Fukuoka 820-8502, Japan

Yusril Yusuf, Yoshiki Hidaka, and Shoichi Kai
Department of Applied Physics, Faculty of Engineering, Kyushu University, Fukuoka 812-8581, Japan
(Received 4 April 2002; published 16 September 2002)

A kind of electrohydrodynamic instability, the prewavy instability, in nematic liquid crystals is reported. The characteristic of the instability was optically investigated and discussed in comparison with some similar instabilities. Obviously the instability partially shows an isotropic feature around the nematic-isotropic transition temperature. Owing to the characteristic properties of the flow and the spatial periodicity, it should be distinguished from a previously proposed isotropic instability.

DOI: 10.1103/PhysRevE.66.031705 PACS number(s): 61.30.−v, 47.20.Lz

I. INTRODUCTION

ac-driven electrohydrodynamic instability in liquid crystals is one of the prime examples of the physics of pattern formation in dissipative systems out of equilibrium. It provides us with a rich variety of stationary and nonstationary patterns that have been intensively studied for the last three decades [1,2]. A primary electroconvection, Williams domain (WD), at a threshold field is found due to the so-called Carr-Helfrich instability [3–5]. Increasing the electric field and changing its frequency, one also observes various secondary instabilities such as the zigzag instability, the Eckhaus instability, the abnormal roll instability, and so on [6–10].

In the present paper we report a kind of instability called the prewavy instability [11] observed in a nematic liquid crystal, and discuss its characteristic in comparison with some similar instabilities [12–18]. Though the prewavy and similar instabilities were already observed and discussed in experiment and theory [13,15–19], open questions and discrepancies still remain. Well-ordered stripe patterns such as the present prewavy pattern were optically observed slightly above the threshold field. In fact the optical stripe patterns due to the prewavy instability may be very similar to wide domains formed by the anisotropic inertia mode instability reported before [14,15]. In contrast to this, observation of mass flows in the prewavy pattern around the nematic-isotropic transition temperature shows a similarity with an isotropic electrolyte mode [12,16]. Sometimes, this isotropic mode cannot be distinguished from the anisotropic dielectric mode observed above a certain high frequency f_c, i.e., cutoff frequency [12,16]. From these reasons the prewavy instability, which is not well understood yet, might be confused with abovementioned instabilities.

The aim of this paper is to clarify the difference of the prewavy instability from other similar instabilities, and to propose a possible mechanism based on experimental results. We argue about the main features of the prewavy instability, i.e., the frequency dependence on the threshold voltage with varying the electric conductivity, the voltage and the frequency dependence on the characteristic wavelength, the geometry of the flows, and the behavior of the threshold voltage around the nematic-isotropic transition temperature.

II. EXPERIMENT

The experimental investigation was performed on sandwich-type cells whose surfaces were coated with transparent electrodes (indium tin oxide). The electric conductivity of a nematic liquid crystal MBBA (p-methoxybenzilidene-p'-n-butylaniline), was controlled by doping with TBAB (tetra-n-butyle-ammonium bromide). An alternating electric field $E=E_0\cos(2\pi ft)$ was applied perpendicularly to the electrodes [$\mathbf{E}=(0,0,\pm E_z)$]. The thickness ($d=20$–250 μm) of a nematic slab with lateral (active) size 1×1 cm^2 was controlled by a polymer spacer (Mylar). The temperature of the cells was stabilized with an accuracy of ± 0.2 °C in a hot stage, which was controlled by an electric control system (Digital Controller DB500). The patterns were observed in the xy plane parallel to electrodes by use of a charge-coupled-device camera (SONY XC-75) mounted on a polarizer microscope (Nikon). In order to investigate flows, small particles [Micropearl (Sekisui Chemical) of diameter 3.88 μm] were introduced into liquid crystal cells. The threshold voltages and the wavelength of patterns were measured with an accuracy of $\pm 5\%$ with an electric multimeter and an optical micrometer, respectively.

III. RESULTS

A. The optical characteristics

A typical prewavy pattern appears in a homeotropic alignment cell, as shown in Fig. 1(a). It is well ordered with a characteristic spatial period $\lambda_w(>4d)$ much larger than the normal convective roll period $\lambda_{WD}(\sim d)$. It is also characterized by the director modulation in the xy plane (due to the in-plane rotation of the director), so that one can distinguish it from a WD with the director modulation in the xz plane. The in-plane rotation of the director was developed by the prewavy instability following the Fréedericksz transition (at 3.5 V). For the sake of convenience we define the x axis parallel to an in-plane orientation of the director in the Fréedericksz state, which is spontaneously selected in the homeotropic cell. In the prewavy patterns the in-plane rotation angle α of the director with respect to the x axis ($\alpha=0$) increased with increasing voltage $V(>V_w)$; see below), and

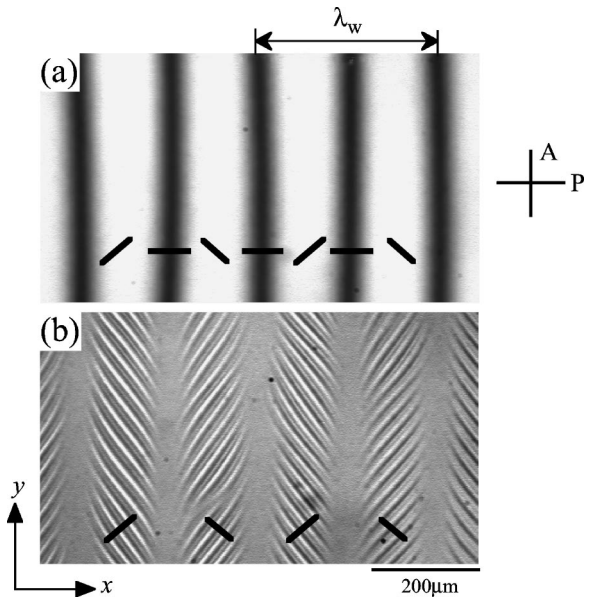

FIG. 1. (a) A typical prewavy pattern in cross polarizers ($V=80.8$ V and $f=1300$ Hz) in a homeotropic cell ($d=49$ μm, $\sigma_{\parallel}=2.36\times10^{-7}\Omega^{-1}$ m^{-1}, and $\epsilon_{\parallel}=4.83$). One of the polarizers was set parallel to the director (black bars) in the dark domains. The cross in the right-hand part means cross polarizers and their orientation, and the black bars in the picture correspond to the directors in the domains. Here the director is a unit vector, which is defined as the locally averaged orientation of the rodlike molecules of nematics. λ_w is the characteristic wavelength of the prewavy pattern. (b) A typical defect-free chevron (DFC) ($V=150$ V and $f=1300$ Hz) developed from (a). This is a convective roll pattern superimposed on the prewavy pattern (a).

saturated to a maximum angle $\alpha_{\max}(\sim45°)$. The detail of $\alpha(V)$ was reported in our previous paper [21]. Only due to the in-plane rotation of the director, no prewavy pattern is detectable without two polarizers. The cross polarizers give us the best contrast of the prewavy pattern, as seen in Fig. 1(a), while it remains visible with parallel polarizers [22].

Increasing voltage at a fixed frequency f ($>f_w$, see below), one can observe a chevron pattern, defect-free chevron [DFC, Fig. 1(b)] [23], characterized by a double periodicity. The DFC is also a typical pattern, in which electroconvective rolls (WD) are superimposed on the prewavy pattern [11,22]. Notice also that the alternating zig and zag rolls of the DFC always form their axes normal to the corresponding in-plane directors, as seen in Fig. 1(b). This chevron pattern is detectable in one or two polarizer(s) and even removing them.

B. The frequency dependence of the threshold voltage

The frequency dependence on the threshold voltage of the prewavy instability was investigated in three (homeotropic) cells with different electric conductivity σ, because the threshold of such an electric instability usually depends on σ. Figure 2 shows the threshold lines (solid circles) of the prewavy pattern above a certain characteristic frequency f_w. The threshold V_w of the prewavy instability weakly depends on f in all cells [20]. Near $f_c[=O(\tau_\sigma^{-1})\sim180$ Hz] in cell 1 with low σ when increasing V, there appears a dielectric

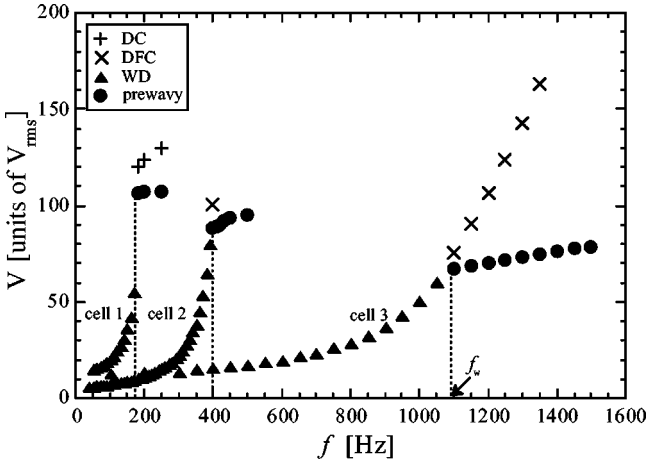

FIG. 2. The phase diagram in the frequency and voltage plane investigated in homeotropic cells with different electric conductivity (cell 1: $\sigma_{\parallel}=3.40\times10^{-8}\Omega^{-1}$ m^{-1}, cell 2: $\sigma_{\parallel}=5.10\times10^{-8}\Omega^{-1}$ m^{-1}, cell 3: $\sigma_{\parallel}=2.36\times10^{-7}\Omega^{-1}m^{-1}$), and same d ($=50\pm5$ μm). Here f_w indicates a characteristic frequency for the prewavy instability.

chevron (DC) instead of the DFC at a threshold voltage after appearance of the prewavy patterns. Here τ_σ corresponds to the charge relaxation time ($\sim10^{-2}$ s). In Fig. 2, moreover, the prewavy pattern begins to appear in lower V and higher f with the increase of σ.

C. The periodicity with respect to frequency and voltage

When a characteristic wavelength λ_w of the prewavy pattern was defined in Fig. 1(a), f and V dependence of λ_w was measured, as shown in Fig. 3. $\lambda_w(f)$ at a fixed V ($=60.1$ V) and $\lambda_w(V)$ at a fixed f ($=2100$ Hz) are almost constant within experimental scatters. Here λ_w is around $6d$. No change of $\lambda_w(f)$ was confirmed in a range from $f=1500$ Hz to 10 kHz. $\lambda_w(V)$ was also independent of V

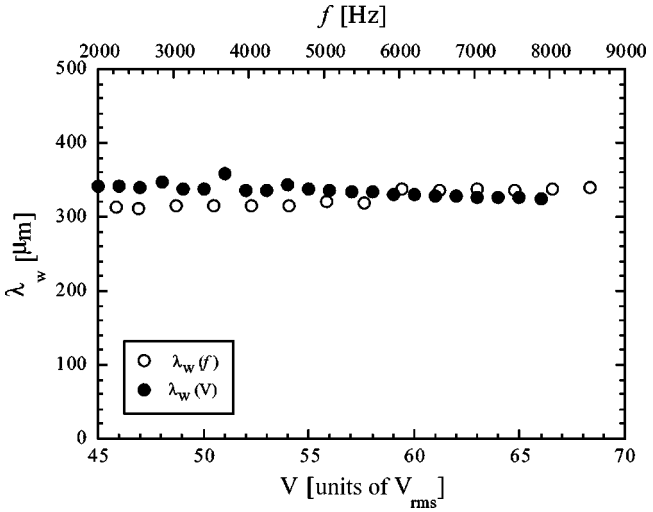

FIG. 3. The characteristic wavelength λ_w of the prewavy pattern. $\lambda_w(f)$ at a fixed $V=60.1$ V and $\lambda_w(V)$ at a fixed $f=2100$ Hz were measured in a homeotropic cell ($d=54.7\mu$m).

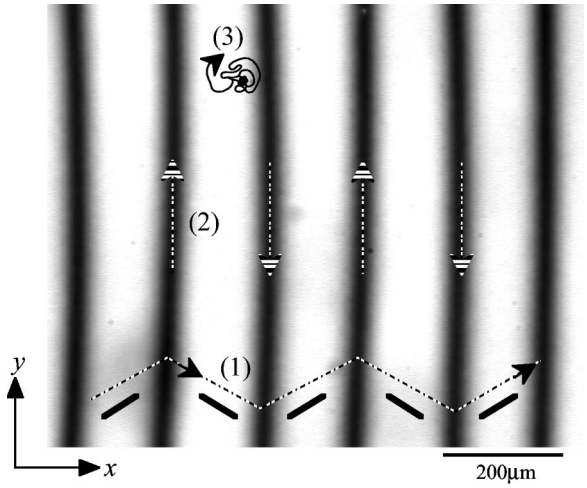

FIG. 4. The trajectory of the particles in the prewavy pattern. (1) The main flow with zigzag trajectory cross the stripes, i.e., along the director. (2) The long circular flow along the stripes. (3) The rolling and rotating motion of a lump of particles. The bars in the picture correspond to the directors in the domains.

below a certain threshold voltage V_{wavy} at which it evolved to a sinusoidal wavy pattern with remarkable change of λ_w [20]. For all cells of planar and homeotropic alignments with different d, no f and V dependence of λ_w were observed below V_{wavy}. λ_w was always measured in the range of $5 \pm 1d$.

D. The flows accompanied with the instability

Since the flow is important to understand the mechanism of electrohydrodynamic instabilities, it was carefully investigated by introducing small particles into a cell. The flow optically observed in the prewavy pattern showed three figures with respect to the trajectory of the particles. (1) The particles moved along the director orientation, that is, they moved zigzag cross the stripes, as shown in Fig. 4. And the flow with the opposite direction was also observed on a different focus plane. Obviously, this is a main flow in the prewavy pattern. (2) Sometimes some of them moved in mutually opposite directions along the stripes on a same focus plane. It seemed to be a long circular flow in the xy plane. (3) Rolling and rotating of a lump of particles was often observed. The particles also moved at voltages below the threshold V_w of the prewavy instability. In this case their trajectory was not totally random and lay along the x direction with large scatters as shown in Fig. 5(a). Above V_w the velocity of the y direction v_y is clearly split as seen in Fig. 5(b). This means that the particles move zigzag cross the stripes in the prewavy pattern, that is, they move along the director modulated periodically by the prewavy instability.

The feature of the main (zig and zag) flow in the prewavy pattern was quantitatively investigated. We defined an angle β characterizing the flow direction, i.e., an in-plane angle between the flow direction and the x axis. The investigation was carried out with observing the motion of 50 particles that were selected randomly in a cell. The particles started to move about 55 V (V_f in Fig. 6). The averaged angle $\overline{\beta}$ was

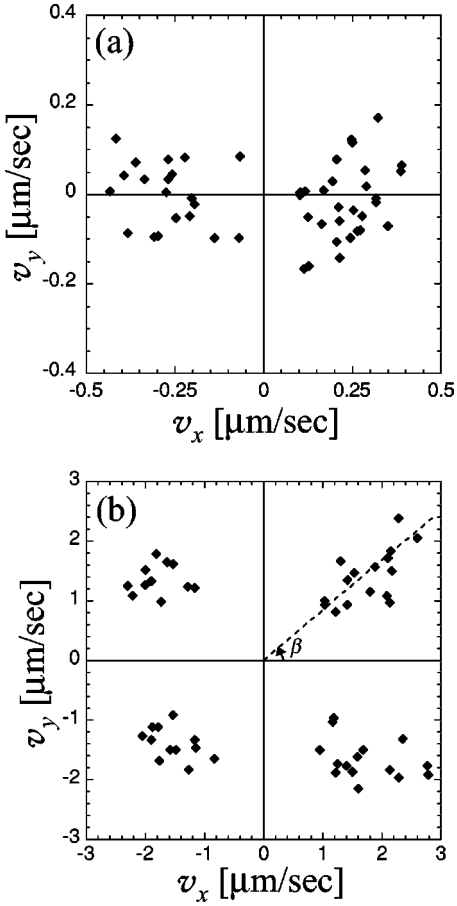

FIG. 5. The flow direction below [(a) $V=55.2$ V] and above [(b) $V=125.2$ V] V_w at a fixed frequency $f=1600$ Hz. Above V_w the velocity of the y direction v_y is clearly split. This means that the particles moved zigzag cross the stripes in the prewavy pattern.

measured as a function of V in Fig. 6. The $\overline{\beta}(V)$ curve indicates a bifurcation. Above V_w ($\sim$84 V) the flow profile seems to be regular and shows zig and zag flow. Below V_w, one can see that $\beta=0$ and has larger standard deviation. The behavior of $\overline{\beta}(V)$ and its amplitude on V are very similar to $\alpha(V)$, the in-plane rotation angle of the director (see Ref. [21]). This means that above V_w the direction of the flow is always parallel to the in-plane director in the prewavy pattern.

E. The temperature dependence of the threshold voltage

The temperature-dependence of V_w was investigated with increasing temperature T. By measuring the threshold value of the optical pattern and the prewavy flows simultaneously, V_w was determined with an accuracy of $\pm 5\%$. Figure 7 shows that $V_w(T)$ decreases monotonously to the nematic-isotropic temperature T_c ($\varepsilon_T=0$). Here $\varepsilon_T(=T-T_c)$ is a relative temperature from T_c. Then the optical (prewavy) pattern disappeared just beyond T_c, but the flow still remained. Obviously, V_w ($\varepsilon_T<0$) continues to the threshold of the flow in the isotropic phase ($\varepsilon_T>0$) without abrupt change. In this isotropic phase ($\varepsilon_T>0$) a lump of the particles observed in the prewavy pattern ($\varepsilon_T<0$) still rolled

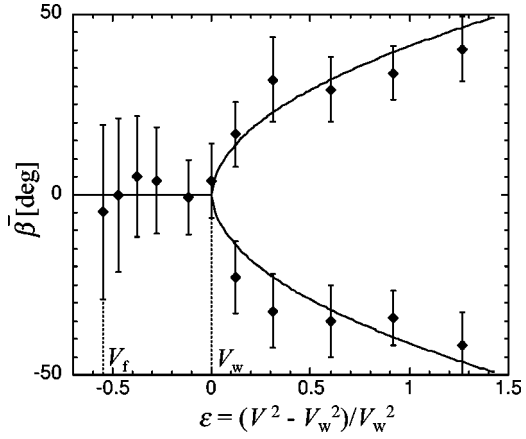

FIG. 6. The flow direction with increasing voltage at a fixed frequency $f=1600$ Hz. An average angle $\bar{\beta}(V)$ between the flow direction and the x axis was measured . Above V_w $\bar{\beta}$ was averaged in zig ($\beta>0$) and in zag ($\beta<0$), respectively. The $\bar{\beta}$ curve indicates a bifurcation (see the text).

and rotated, and almost of the single particles moved randomly in the xy plane. On the other hand, the thresholds of WD, DFC, and DC diverge at T_c ($\varepsilon_T=0$), because they are all anisotropy-originated modes in the nematic phase.

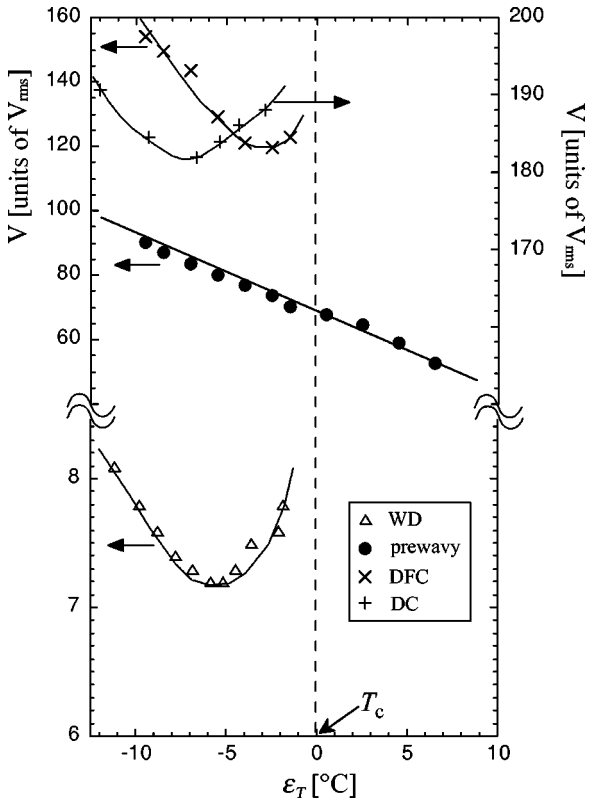

FIG. 7. The behavior of electric instabilities around the nematic-isotropic transition temperature T_c. The threshold of the prewavy instability (solid circles) continues around $T_c(\varepsilon_T=0)$, while those of WD, DFC, and DC all diverge at T_c. A relative temperature $\varepsilon_T(=T-T_c)$ is used because of the small difference of T_c on each cell. The thin lines are a guide for the eye.

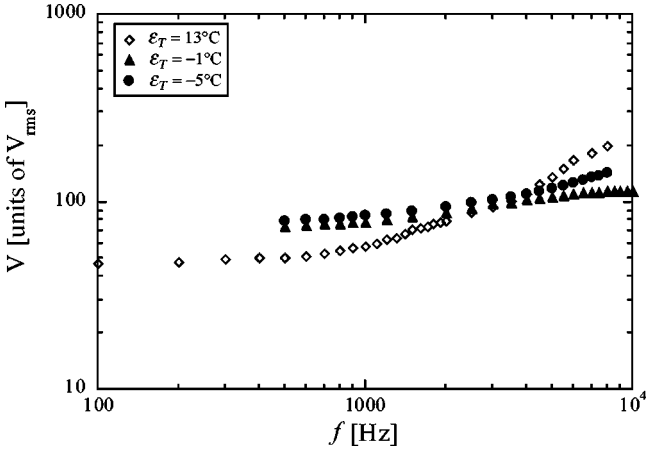

FIG. 8. The threshold voltage $V_w(f)$ in nematic and isotropic phases. $V_w(f)$ in the isotropic phase ($\varepsilon_T=13$°C) shows a similar behavior to that in the nematic phase near ($\varepsilon_T=-1$°C) and far ($\varepsilon_T=-5$°C) T_c.

In addition, the frequency dependence of V_w in the isotropic phase ($\varepsilon_T>0$) was measured, in order to compare with $V_w(f)$ in the nematic phase ($\varepsilon_T<0$). It shows a plateau at low frequencies and smooth increase of V_w with increasing f, as seen in Fig. 8. This behavior of $V_w(f)$ does not change below and above T_c. In this measurement $V_w(f)$ below $T_c(\varepsilon_T<0)$ was determined by the optical pattern and the flow, while it was done only by the flow (rolling or rotating) above $T_c(\varepsilon_T>0)$.

IV. DISCUSSION AND CONCLUSION

In order to classify the prewavy instability observed at a high frequency regime ($f>f_w$), it should be compared to the previously proposed ones such as the dielectric, inertia, and isotropic (electrolyte) modes that were also observed in high frequencies. There are a lot of similarities between the prewavy and inertia mode with regard to the optical patterns and the frequency dependence of the threshold voltage, as described Secs. III A and III B. However, the inertia as well as the dielectric mode was known as an anisotropic mode that could appear only in the (anisotropic) nematic phase [15,16]. Their modes always show a distinct divergence at the nematic-isotropic transition temperature T_c, as shown in Fig. 7 (see DC) and Fig. 7 in Ref. [15]) while the prewavy instability continues around T_c. In addition, no dependence of the prewavy wavelength (λ_w) with respect to voltage and frequency in Fig. 3 also distinguishes the prewavy instability from the dielectric, inertia, and isotropic (electrolyte) modes [25]. We summarize these differences in Table I to compare easier.

On the other hand, the prewavy instability shows some difference from the isotropic (electrolyte) mode proposed previously [12,16,25], though both have a continuity of the threshold of the flow around T_c. Compared to Refs. [12,13,16], the most different feature is the trajectory of the flows. According to their isotropic mode, the vortices of the particles were a main flow in nematic phase with their

TABLE I. Comparison between the present prewavy mode and other similar modes at high frequencies.

	Dielectric mode	Inertia mode	Isotropic mode	Prewavy mode
$V_{th}(f)$	$\sim f^{1/2}$	$\sim f^{c(\sigma)}$	$\sim f^{1/2}$	$\sim f$
$\lambda_{th}(f)$	$\sim f^{-1/2}$	$\sim 3d$	$\sim f^{-1/2}$	$4d-6d$
$\lambda_{th}(V)$	$-$	$\sim 3d(V<V'), \sim V^{-2}(V>V')$[a]		$4d-6d$
$V_{th}(T)$	$V_{th}(T=T_c)\to\infty$	$V_{th}(T=T_c)\to\infty$	$V_{th}(T=T_c)=V_c(f)$	$V_{th}(T=T_c)=V_c(f)$
flow	small surface flow	long circular flow	convective flow	zig-zag flow, long circular flow, rolling/rotating flow
Refs.	[12,13,16,23,24]	[14,15,17,18,24]	[12,13,16,23,24]	[11,19,20,21]

[a]Also $\lambda_{th}(V)\sim\lambda_{th}(V=V_{th})-aV$ in Ref. [11].

size of order of cell thickness, but no zigzag and long circular flows [(1) and (2) of the prewavy flows in Fig. 4] were observed. Moreover, no (isotropic-type) wide stripe pattern such as the present prewavy pattern has been reported. Thus, the prewavy instability should be classified as a different type of isotropic mode. In case of the previous isotropic mode, moreover, the frequency dependence of the wavelength of the corresponding pattern in liquid crystals was known to be $\lambda_{th}(f)\sim f^{-1/2}$ at threshold voltages [24,25]. This is also totally different from our result that shows no frequency dependence of λ_w in the prewavy pattern (see Fig. 3 and Table I).

In principle, the previous isotropic mode is induced in a thin layer near electrodes due to an inhomogeneity of the charge carrier density $q(z)$ along the z axis. Such an inhomogeneity can be possible by an electrolysis in a liquid crystal. Then positive and negative charges drift, respectively, to the negative and positive electrodes when applying an ac field across electrodes. Increasing frequency above a certain characteristic frequency, the charges will cross only a part of thin layer thickness. These charges oscillating along the z axis can induce a flow near the electrodes at sufficiently high voltages. In this case vortices are expected to form in both thin layers near the electrodes [24,25]. From this instability model, however, it is impossible to expect our large prewavy domains and the characteristic flow in the prewavy pattern.

In conclusion, the present prewavy instability should be classified as a different type of isotropic mode distinguishable from the other high-frequency modes. Here a coupling model between the isotropy-originated flow described above and the director might be considered to understand the prewavy instability. Namely, the strongly developed flow at high voltages could induce an inhomogeneous (twist) Freedericksz transition (e.g., see Ref. [26]), i.e., the prewavy instability. Moreover, the large wavelength of the prewavy patterns could be formed by the elastic constants and viscous coefficients of the liquid crystal [26]. The wavy and spiral wavy patterns successively evolved from the prewavy pattern are also an interesting subject to understand the nature of pattern formation in dissipative systems [19,20].

ACKNOWLEDGMENTS

The authors thank W. Pesch, L. Kramer, A. Buka, N. Eber, and T. Toth-Katona for valuable discussions and comments. This work was partly supported by a Grant-in-Aid for Scientific Research from the Ministry of Education, Science, Sports and Culture in Japan (Grant Nos. 13750017,10440117, 12740238, 14340123, and 14740239).

[1] L. Kramer and W. Pesch, Annu. Rev. Fluid Mech. **27**, 515 (1995).
[2] S. Kai and W. Zimmermann, Prog. Theor. Phys. Suppl. **99**, 458 (1989).
[3] R. Willams, J. Chem. Phys. **39**, 384 (1963).
[4] E.F. Carr, Mol. Cryst. Liq. Cryst. **7**, 253 (1969).
[5] W. Helfrich, J. Chem. Phys. **51**, 4062 (1969).
[6] M.C. Cross and P.C. Hohenberg, Rev. Mod. Phys. **65**, 851 (1993).
[7] H. Richter, A. Buka, and I. Rehberg, Mol. Cryst. Liq. Cryst. **251**, 181 (1994).
[8] E. Plaut, W. Decker, A.G. Rossberg, L. Kramer, W. Pesch, A. Belaidi, and R. Ribotta, Phys. Rev. Lett. **79**, 2367 (1997).
[9] J.-H. Huh, Y. Hidaka, and S. Kai, Phys. Rev. E **58**, 7355 (1998).
[10] J.-H. Huh, Y. Hidaka, and S. Kai, Mol. Cryst. Liq. Cryst. **328**, 497 (1999).
[11] J.-H. Huh, Y. Hidaka, A.G. Rossberg, and S. Kai, Phys. Rev. E **61**, 2769 (2000).
[12] M.I. Barnik, L.M. Blinov, M.F. Grebenkin, and A.N. Trufanov, Mol. Cryst. Liq. Cryst. **37**, 47 (1976).
[13] M.I. Barnik, L.M. Blinov, S.A. Pikin, and A.N. Trufanov, Zh. Éksp. Teor. Fiz. **72**, 756 (1977) [Sov. Phys. JETP **45**, 396 (1977)].
[14] P. Petrescu and M. Giurgea, Phys. Lett. **59A**, 41 (1976).
[15] A.N. Trufanov, L.M. Blinov, and M.I. Barnik, Zh. Éksp. Teor. Fiz. **78**, 622 (1980) [Sov. Phys. JETP **51**, 314 (1980)].
[16] R. Ribotta and G. Durand, J. Phys. (Paris), Colloq. **C3**, 334 (1979).
[17] S.A. Pikin and V.G. Chigrinov, Zh. Éksp. Teor. Fiz. **78**, 246

(1980) [Sov. Phys. JETP **51**, 123 (1980)].
[18] L. Nasta, A. Lupu, and M. Giurgea, Mol. Cryst. Liq. Cryst. **71**, 65 (1981).
[19] S. Kai and K. Hirakawa, Solid State Commun. **18**, 1573 (1976).
[20] S. Kai, Y. Adachi, and S. Nasuno, *Spatio-Temporal Patterns*, edited by P.E. Cladis and Palffy-Muhoray (Addison-Wesley, New York, 1995), p. 313.
[21] J.-H. Huh, Y. Hidaka, Y. Yusuf, N. Eber, T. Toth-Katona, A. Buka, and S. Kai, Mol. Cryst. Liq. Cryst. **364**, 111 (2001).
[22] J.-H. Huh, Y. Hidaka, and S. Kai, Mol. Cryst. Liq. Cryst. **366**, 2685 (2001).
[23] In order to distinguish the chevron pattern in Fig. 1(b) from a defect-mediated chevron, we named the defect-free chevron (DFC) for Fig. 1(b). See Ref. [11] for the details.
[24] L.M. Blinov, Sci. Prog., Oxford **70**, 263 (1986).
[25] L.M. Blinov and V.G. Chigrinov, *Electrooptic Effects in Liquid Crystal Materials* (Springer-Verlag, New York, 1994).
[26] F. Lonberg and R.B. Meyer, Phys. Rev. Lett. **55**, 718 (1985).